Internship Report

Analysis of infrared thermography data from edge probe experiments at the W7-X stellarator

Aloïs Coquillard

Département de Physique, M1 SdM

École Normale Supérieure de Lyon

Année 2025–2026

Carried out at

Max Planck Institut

Für Plasmaphysik

Teilinstitut Greifswald

Wendelsteinstraße 1

https://www.ipp.mpg.de

Supervised by

Carsten Killer

Stellarator-Dynamik

Plasma Turbulence

tel. 03834 88 2228

carsten.killer@ipp.mpg.de

Abstract

The objective of this internship was to study an infrared camera view of the Langmuir probe **Fluc 3** inside the W7-X stellarator in order to model thermal absorption by the probe tips and insulation, and compare the inferred heat fluxes with direct Langmuir probe measurements.

Keywords: *Langmuir probe, infrared thermography, thermal modeling, stellarator, W7-X, heat flux*

I. Acknowledgements

Je tiens à remercier Carsten Killer pour m'avoir accueilli dans son équipe et encadré tout au long de ce stage, ainsi que l'ensemble de l'équipe Stellarator-Dynamik de l'IPP Greifswald pour leur disponibilité et les discussions enrichissantes. Je remercie également l'École Normale Supérieure de Lyon et le département de physique pour m'avoir permis d'effectuer ce stage dans le cadre du master M1 SdM.

Contents

II. Introduction

Plasma, often referred to as the fourth state of matter, is widely studied due to its many applications, notably in nuclear fusion. Controlled fusion would enable the production of clean and sustainable energy by reproducing the processes occurring in the Sun. Despite decades of progress and major international efforts such as ITER, achieving efficient and stable fusion remains a major scientific challenge.

A key difficulty lies in plasma stability. Even when appearing stable, plasmas are affected by small-scale instabilities that can lead to turbulence and degrade confinement. In tokamaks, these effects can result in disruptions, causing a sudden and violent loss of confinement.

Stellarators offer an alternative approach, relying entirely on externally generated magnetic fields and thus avoiding large plasma currents. This makes them inherently more stable and suitable for steady-state operation. The Wendelstein 7-X (W7-X) stellarator, located at the Max Planck Institute for Plasma Physics in Greifswald, is the world's largest optimized stellarator and a leading experiment in this field, aiming to demonstrate that optimized magnetic configurations can achieve high-performance, steady-state confinement.

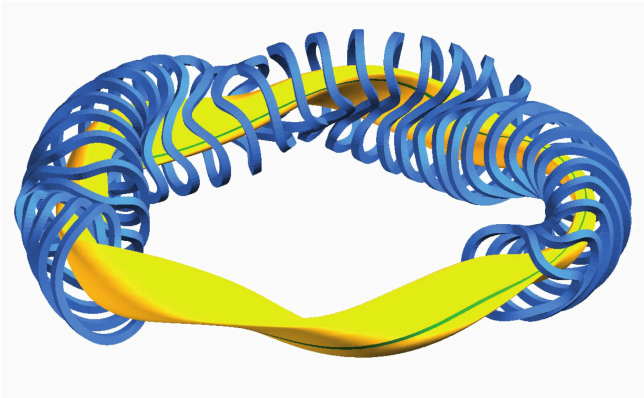

Figure 1: The Wendelstein 7-X stellarator at IPP Greifswald.

In this context, studying plasma edge physics and transport processes is essential for improving confinement and understanding plasma–wall interactions, which are critical for the development of future fusion reactors. Diagnosing the plasma edge requires dedicated probes that can withstand the harsh environment and provide local measurements of electron temperature, density, and heat flux.

The goal of this internship was to develop an analysis pipeline for the infrared (IR) camera that observes the **IPP Fluc 3** multipin Langmuir probe during plasma experiments at W7-X. By extracting thermal signals from the camera video and modeling the heat conduction in the probe pins, we aim to infer the local heat flux deposited by the plasma and compare it to the Bohm heat flux estimated from the Langmuir probe measurements themselves. This cross-validation is essential to understand the reliability of both diagnostics and to study the spatial and temporal structure of heat deposition in the divertor region.

III. The Fluc3 Probe and Divertor Thermal Cameras

III.I. The IPP Fluc3 Multipin Langmuir Probe

The IPP Fluc 3 is a multipin Langmuir probe designed to measure local plasma parameters — electron temperature T_e, electron density n_e, and ion saturation current I_{sat} — in the edge plasma of W7-X, specifically within the divertor island region. It is mounted on the Multi-Purpose Manipulator (MPM), a pneumatic arm that inserts the probe radially into the plasma on a shot-by-shot basis, performing a rapid plunge of typically a few hundred milliseconds.

The probe head carries 29 electrically independent pins arranged on its surface, grouped in triples to enable triple-probe measurements. In a triple-probe configuration, one pin is biased positively, one negatively, and one is left floating, allowing simultaneous estimation of T_e and I_{sat} without the need for a voltage sweep. The Bohm heat flux Q_{Bohm} is then inferred as:

$$Q_{\mathrm{Bohm}} = k_B T_e n_e c_s$$

where $c_s = \sqrt{k_B \frac{T_e}{m_i}}$ is the Bohm velocity and m_i is the ion mass.

Figure: photograph of the Fluc3 probe head showing the 29 pins and triple-probe grouping.

Figure 2: Figure: photograph of the Fluc3 probe head showing the 29 pins and triple-probe grouping.

A key challenge for interpreting the measurements is that the heat flux impinging on the probe is not always perpendicular to the probe face. The orientation of field lines relative to the probe surface depends on the magnetic configuration of W7-X, which can be varied via external coils. This means that the effective heat-flux projection onto the probe pins changes between experimental scenarios, making a purely Langmuir-based heat flux estimate sensitive to the assumed geometry.

Figure: schematic of heat flux angle relative to probe face for different W7-X magnetic configurations.

Figure 3: Figure: schematic of heat flux angle relative to probe face for different W7-X magnetic configurations.

III.II. The QHW Infrared Camera

The QHW camera is a thermal infrared camera providing a direct view of the Fluc3 probe head during plasma plunges. It is based on an uncooled microbolometer sensor with a native frame rate of up to 50 fps, though in practice the current experimental setup limits acquisition to approximately 12 fps due to USB bandwidth constraints. The sensor resolution is 640 × 512 pixels. Images are stored as raw 16-bit unsigned integers (uint16), with no factory-provided intensity-to-temperature calibration.

The camera is mounted at an angle of approximately 36° to the probe axis, giving a sideways view that is well suited for observing the probe face but introduces a perspective distortion that must be corrected before pin-level analysis. The camera optics include an AEF41 spectral filter, which defines the effective sensitivity band and must be accounted for in the radiometric calibration.

Figure: raw QHW camera frame showing the Fluc3 probe at a typical plunge position.

Figure 4: Figure: raw QHW camera frame showing the Fluc3 probe at a typical plunge position.

A notable characteristic of the camera is the presence of an internal temporal frame averager, which smooths consecutive frames to reduce noise. While this improves image quality during static conditions, it introduces artifacts during rapid probe motion: as the probe moves, the averager mixes frames from different probe positions, producing blurred and thermally inaccurate images. This effect was initially attributed to automatic gain control (AGC) but further investigation showed that AGC was not active; the temporal averager is the sole source of these motion artifacts. Frames acquired during probe motion must therefore be excluded from thermal analysis or reconstructed by interpolation.

IV. IR Camera Video Analysis

The extraction of per-pin temperature time series from the raw QHW camera video involves several successive processing steps, each addressing a specific technical challenge. The full pipeline is implemented in Python and organized as a set of notebooks and supporting modules, versioned in the project repository.

IV.I. Video Synchronization and Temperature Calibration

IV.I.I. Time synchronization

The first step is to align the camera timestamps with the probe arm position data stored in the W7-X archive database. This synchronization is necessary to know, for each camera frame, the exact radial position of the probe head in the vacuum vessel.

An analysis of the camera internal pipeline revealed a systematic offset: the timestamp recorded in the database is consistently 43 ± 2 ms later than the actual time of image capture, with a small shot-to-shot fluctuation. This offset arises from the camera's internal image processing delay. Once corrected, the horizontal synchronization between camera frames and probe position is accurate to within the frame interval (80 ms at 12 fps).

Figure: probe arm position vs time, before and after timestamp correction, showing horizontal alignment.

Figure 5: Figure: probe arm position vs time, before and after timestamp correction, showing horizontal alignment.

The rotation and crop parameters — angle, center position, scale — are stored in `Fluc3parameters.py` at the repository root and differ between the OP2.2 and OP2.3 experimental campaigns, reflecting changes in the camera mounting between campaigns.

IV.I.II. Temperature calibration

The QHW camera outputs raw 16-bit ADU (analog-to-digital unit) values that must be converted to physical temperature. The previous calibration (Ian Martin Hundt) used a linear fit derived from blackbody measurements, valid only in the 400–500°C range. However, during normal plunge experiments the probe surface temperature rises to at most approximately 350°C (623 K), placing it entirely outside the range where the linear calibration is reliable.

The calibration developed during this internship uses a per-day, reciprocal polynomial approach: for each experimental day, a reference shot is used to compute strike-line masks that isolate the plasma-facing surface from background. A batch of reference shots is then accumulated to construct a day-specific ADU-to-Kelvin conversion polynomial. This day-by-day approach accounts for camera drift between sessions, which can be significant over a multi-week campaign.

Figure: example calibration curve (ADU vs K) for a reference day, with polynomial fit and residuals.

Figure 6: Figure: example calibration curve (ADU vs K) for a reference day, with polynomial fit and residuals.

Because the temporal frame averager corrupts frames acquired during probe motion, the raw temperature time series for each pin contains gaps around the motion segments. These gaps are filled by Legendre polynomial interpolation applied to the reliable (stable-probe) segments on either side, while preserving the high-temperature data that is most physically meaningful.

IV.II. Probe 3D Geometry to 2D Video Projection

To associate each camera pixel with a specific probe pin, a geometric mapping from the 3D probe model to the 2D camera image plane is required. The probe geometry is described by a 3D STL mesh (`fluc3_body.stl`) that models the probe head with its 29 pin locations in W7-X machine coordinates.

The mapping is performed in two steps. First, a 3D-to-2D projection is computed using the known camera viewing angle and position relative to the probe, producing the expected pixel coordinates of each pin edge and corner in the camera image. This projection is implemented in `geometry_utils.py` and visualized interactively with a correspondence tool (`correspondance_tool.py`) that allows manual fine-tuning of the camera pose parameters.

Figure: 3D STL model of the Fluc3 probe head with the 29 pins highlighted.

Figure 7: Figure: 3D STL model of the Fluc3 probe head with the 29 pins highlighted.

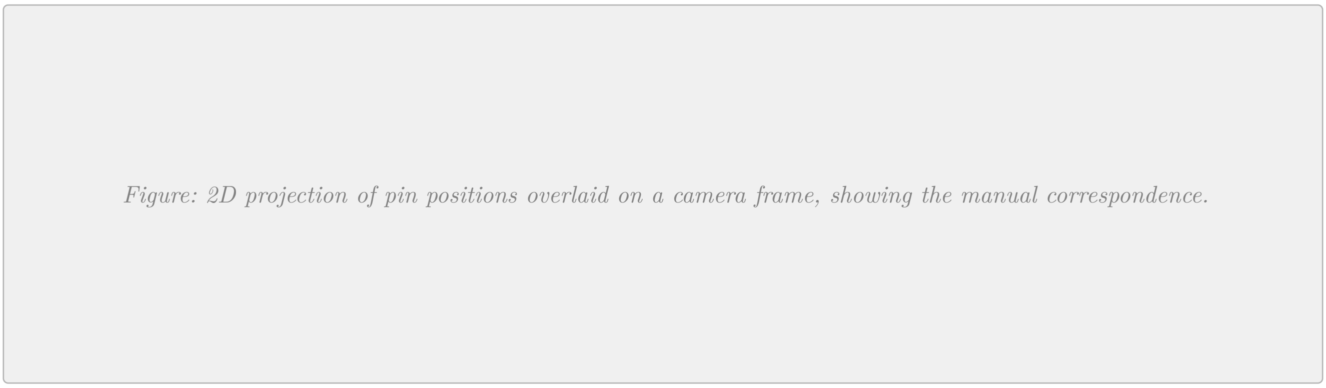

Figure 8: Figure: 2D projection of pin positions overlaid on a camera frame, showing the manual correspondence.

The result is a CSV file (`probe_pin_projection.csv`) containing the pixel coordinates of each of the 29 pins for each experimental campaign. These coordinates are then used to extract per-pin intensity time series from the stabilized video, by averaging over the pixel region corresponding to each pin.

IV.III. Video Stabilization: the Lucas-Kanade Algorithm

Even after timestamp correction and rotation, the probe image still exhibits residual motion artifacts: mechanical vibrations of the arm after each plunge introduce a vertical oscillation, while imperfect time synchronization causes a small horizontal drift during motion. These residual shifts must be corrected before pin-level intensity extraction, since a one-pixel error in pin position corresponds to a non-negligible temperature error given the small pin size relative to camera resolution.

Stabilization of thermal infrared video is inherently difficult for several reasons specific to this setup: the probe surface has no consistent intensity pattern (it heats and cools during the plunge), its apparent shape changes as it rotates with the arm, and contrast is sometimes very poor during the coldest phases. Algorithms based on cross- correlation or template matching were tested but proved insufficiently robust.

The most effective approach was found to be the Lucas-Kanade (LK) sparse optical flow algorithm, applied selectively to stable probe segments — phases where the probe is stationary or moving very slowly. The LK algorithm tracks a sparse set of feature points between consecutive frames and estimates the inter-frame rigid displacement (translation only). The estimated shifts are then interpolated across motion segments using the stable- segment estimates as boundary conditions.

Figure 9: Figure: stabilization result — side-by-side before/after comparison for a representative plunge segment.

V. Heat Flux Estimation

V.I. A Simple 1D Thermal Conduction Model

Once per-pin temperature time series are available, the goal is to infer the local heat flux deposited on each pin by the plasma. A simple 1D thermal model was developed for this purpose, based on the following assumptions:

- The probe internal body acts as a heat reservoir (thermal bath) at a slowly varying background temperature T_{body}.
- Each pin is thermally isolated from its neighbors (no lateral heat flow between pins).
- The pin material is homogeneous and isotropic.
- The thermal conductivity of the pin material is much smaller than that of the probe body, so the pin–body interface is the dominant thermal resistance.
- The heat flux q deposited on the plasma-facing tip of the pin is approximately constant during each heat-up segment.

Under these assumptions, the pin temperature evolves as:

$$T(t) = T_\infty + (T_0 - T_\infty)e^{-t/\tau}$$

where T_∞ is the equilibrium temperature, T_0 is the initial temperature at the start of the heat-up, and τ is the thermal time constant of the pin. The heat flux is then proportional to the temperature rise:

$$q_W = \rho c \frac{T_\infty - T_0}{\tau}$$

where ρ and c are the density and specific heat capacity of the pin material. In practice, an exponential fit is performed on each identified heat-up segment to extract T_∞, T_0, and τ, and q_W is computed pin by pin and plunge by plunge.

Figure: example per-pin temperature curve during a plunge, with exponential fit overlaid and extracted parameters.

Figure 10: Figure: example per-pin temperature curve during a plunge, with exponential fit overlaid and extracted parameters.

This simple model has known limitations. The camera frame rate of 12 fps means that a typical heat-up burst of 300 ms yields only 2–3 data points, making the exponential fit statistically fragile. For longer heat-up events, the temperature rise is observed to follow a $\left(1 - e^{-t/\tau}\right)$ shape rather than $\sqrt{t}$ as expected for a semi-infinite solid, suggesting that the heat bath assumption is more appropriate than a purely diffusive model in those cases. Additionally, an anomalously rapid temperature decrease is sometimes observed in the first 100 ms of the cooldown phase, likely due to thermal radiation from surface impurity deposits on the pin tips, which are gradually removed over successive plunges (probe cleaning effect).

V.II. Comparison with Langmuir Probe Measurements

The heat flux values inferred from the IR model (q_{IR}) can be compared to the Bohm heat flux (Q_{Bohm}) computed from the triple Langmuir probe measurements stored in the W7-X archive. This comparison serves as a cross-validation of both diagnostics and as a way to probe the agreement between the thermal and electrical measurements of edge plasma transport.

Figure: side-by-side heatmaps of IR heat flux and Bohm heat flux for each of the 29 pins, for a representative plunge.

Figure 11: Figure: side-by-side heatmaps of IR heat flux and Bohm heat flux for each of the 29 pins, for a representative plunge.

Initial comparisons show qualitative agreement in the spatial structure of heat deposition across the probe face, with the highest fluxes concentrated on the plasma-facing pins. However, quantitative agreement requires a more refined calibration of both the temperature calibration (currently in progress for the 270–500 K range) and the thermal model parameters. A 3D ANSYS simulation of the probe under representative thermal boundary conditions is planned to provide a higher-fidelity reference and to guide corrections to the 1D model.

Figure: correlation plot of q_IR vs Q__Bohm across pins and plunges, with identity line.

Figure 12: Figure: correlation plot of q_IR vs Q__Bohm across pins and plunges, with identity line.

VI. Conclusion

This internship resulted in the development of a complete end-to-end pipeline for extracting heat flux information from the QHW infrared camera data at W7-X. Starting from raw 16-bit camera frames and W7-X archive data, the pipeline produces per-pin, per-plunge heat flux estimates for the 29 pins of the Fluc3 probe, as well as side-by-side comparison maps with the Langmuir-derived Bohm heat flux.

The main technical achievements are:

- A robust video processing chain (rotation, cropping, timestamp correction, Lucas-Kanade stabilization) that reliably tracks the probe across full plunge sequences.
- A day-by-day reciprocal polynomial temperature calibration method adapted to the low-temperature operating range of the probe (270–500 K), superseding the previous linear calibration.
- A 3D-to-2D geometric mapping of all 29 probe pins onto the camera image plane.
- A 1D exponential thermal model for per-pin heat flux extraction.
- A first set of IR–Langmuir heat flux comparisons showing qualitative spatial agreement.

Several directions remain open for future work. The temperature calibration needs to be fully validated with an uncertainty analysis over the target temperature range. The 1D thermal model should be cross-validated against a 3D ANSYS finite-element simulation to assess systematic biases. On the hardware side, the camera USB bandwidth limitation (currently 12 fps vs. 50 fps native) should be resolved before the next experimental campaign (OP2.4), together with a final decision on the deactivation of the temporal frame averager, in order to obtain the time resolution needed to resolve individual heat-up events reliably.

More broadly, once the calibration and model are finalized, the pipeline will enable a systematic study of heat flux correlation with magnetic configuration, plasma heating power, and density — key questions for understanding plasma–wall interactions in stellarator divertors and for preparing future high-performance campaigns at W7-X.

This document was written in Typst using Verso, a self-hosted collaborative editor for Typst and Quarto documents created by Aloïs Coquillard, based on Overleaf Community Edition.